

Asymmetric Whirl Combustion: A New Approach for Non-Premixed Low NO_x Gas Turbine Combustor Design

H. Clay Gabler*, Richard A. Yetter†, and Irvin Glassman‡
Princeton University, Princeton, New Jersey 08544

ABSTRACT

A promising new approach for non-premixed low-NO_x combustor design is presented in which fuel was injected off-axis or asymmetrically into a whirl flame. Experiments using this technique to react methane and air in an atmospheric laboratory scale burner demonstrated low NO emissions levels coupled with modest CO emissions. NO emissions below 15 PPM were measured with associated CO below 25 PPM at 15% O₂. The combustor was shown to exhibit unusual stability characteristics even at overall equivalence ratios below $\phi=0.1$. Presented in this paper are the design of the novel whirl combustor, the results of an experimental characterization of the combustor stability, emissions, and combustion efficiency, and an examination of the internal structure of the flame which provides an explanation of this unusual behavior.

INTRODUCTION

Because of their low incremental capital cost, thermodynamic efficiencies exceeding 50% for combined cycle units, and the current low cost of natural gas, stationary gas turbines have become increasingly attractive as power generation devices¹. Continuing research on these devices has led to cycle efficiencies as high as 60% for some advanced combined-cycle units². It has been estimated that in 1990 34,000 MW of gas turbine generating capacity was sold as compared to 23,000 MW for the more traditional steam turbines³.

However, the growth in gas turbine capacity has been accompanied by increasingly stringent environmental regulation of NO_x emissions for gas turbines as well as for other power generating technologies. Among the strictest limits have been NO_x standards in the California South Coast Air

Quality Management District which were set at 15 PPM corrected to 15% O₂.⁴ These regulatory pressures have motivated an active and continuing search for new gas turbine combustor designs which reduce NO_x emissions.

One of the more effective methods of reducing NO formation has been lean premixed combustion⁵. Recent commercial designs have reduced NO_x emission levels below 25 PPM at gas turbine pressures and below 10 PPM at atmospheric pressure^{6,7}. However, lean premixed combustion has not been without drawbacks. First, lean premixed combustion, as currently adopted, requires fuel-air premixing and contributes to the inherent risk of flame flashback in such systems. Second, lean premixed combustion has been noted to suffer from combustion instability. Third, the low combustion temperatures associated with lean premixed combustion often reduced NO emission levels at the expense of increased CO emission levels.

Research at Princeton with whirl flames has produced a promising new concept for combustor design with the potential for low NO_x emission levels⁸. The new design concept has methane and air injected directly into the combustor in a configuration which avoids much of the complexity, safety concerns, and stability problems of other NO control methods, e.g. lean pre-mixed combustion. Presented in this paper are the design of the novel whirl combustor, the results of an experimental characterization of the combustor stability, emissions, and combustion efficiency, and an examination of the internal structure of the flame which provides an explanation of this unusual behavior.

Review of Whirl Flames. Whirl flames are defined as those produced by introducing air with a strong tangential velocity component into a cylindrical combustion chamber to produce a whirling flow field. The fuel in the system described here is injected separately. The air is injected with no axial velocity component. This approach is in contrast to swirl flames in which the air is introduced with a large axial velocity component as well as a rotational component.

This straightforward distinction between swirl and whirl has led to flames with a radically different appearance and method of flame stabilization. While the whirl flame which has been produced can be described as a hollow cylinder with a relatively quiescent center, swirl flames have been characterized

*Graduate Student, Department of Mechanical and Aerospace Engineering.

†Senior Research Scientist, Department of Mechanical and Aerospace Engineering.

‡Professor, Department of Mechanical and Aerospace Engineering, Fellow AIAA.

Copyright © 1998 by the American Institute of Aeronautics and Astronautics, Inc. All rights reserved.

by a vigorously-burning central recirculation zone. This central recirculation zone is produced by vortex breakdown of the strong swirling flow. The recirculation zone has been identified as a flame stabilization mechanism which provides a region of reverse flow where chemical reaction times match flow times, and which serves to transport hot combustion products and enthalpy back toward the inlet ports. Swirl combustion has received considerable prior attention^{9,10}.

Some of the earliest work on whirl flames was presented by Hottel and Person and Albright and Alexander who studied the symmetric injection of gas-phase fuels into a whirl flame^{11,12}. These early studies both injected fuel along the centerline of a whirling flow. Ishizuka¹³ investigated laminar premixed whirl flames, which he referred to as stretched 'tubular flames', created by injecting the fuel-air mixture tangentially at the outer radius of a cylinder. Several researchers have directly injected fuel at the periphery of a swirling flow^{14,15}. However, in contrast to the approach described in this paper, these combustors introduced swirling air with a large axial velocity component and exhausted combustion gases at the end of a duct open to the atmosphere. The resulting flow featured a recirculation zone which mixed hot combustion products with the incoming reactants thereby stabilizing the flame.

New Whirl Combustion Concept. The concept of asymmetric whirl combustion introduced here developed from an attempt to increase the radiant intensity of natural gas by adapting the classic Emmons Fire Whirl technique in which a circular screen is rotated around a circular liquid fuel pool¹⁶. This approach was extended by Chigier by replacing the liquid pool with a gaseous turbulent jet¹⁷. In this approach the longitudinal axis of the screen and fuel jet are coincident and for the purposes here will be called symmetric. The result is an elongation of the fuel jet diffusion flame with greater surface area and luminosity for the same fuel flow.

The rotating screen induced a whirling flow field which produced an adverse pressure gradient from the center of the cylinder to the mesh wall. Under this pressure gradient, the hot, lower density flamelets of the turbulent flame brush were drawn preferentially to the centerline of the cylinder producing a flame of smooth laminar appearance. In the absence of the turbulent flamelets, fuel-air mixing and consumption rates were reduced leading to increased flame height. The observed increase in luminosity was due to the increase of soot formed because of the longer residence time of the methane in the extended flame. Indeed, methane would not soot as a fuel if methyl radicals which form during its pyrolysis did not recombine to form ethane, and start the chain system that leads to soot nucleation¹⁸.

Similar results were achieved without a rotating screen by surrounding the jet with a tall split cylinder so that the longitudinal axes of the cylinder and jet were again coincident or symmetric⁸. A split-cylinder was constructed of two half-cylinders which were oriented in such a way that air was drawn in through the opening between the two half-cylinders by combustion-induced buoyancy to produce a swirling flow. In this split-cylinder configuration, the flame buoyancy induces air. There had been no apparent literature references to this fuel jet, split-cylinder procedure. With the split-cylinder apparatus centered over the fuel jet similar to the rotating screen, the methane-air flame changed from a bright orange squat turbulent flame brush to a bright orange elongated flame of smooth spiral-like appearance.

Most important to the development of the novel combustor was the discovery that displacing the split-cylinder off-axis would cause the flame to self-extinguish. A small displacement of the split-cylinder simply turned the very luminous sooting flame into a small helical slightly luminous blue flame whose axis was displaced from that of the jet exit. Indeed, the helical flame axis was found to be the same as that of the split-cylinder. Slight blowing in the slot opening readily extinguished the flame. However, very surprisingly, under the same small displaced condition, strong blowing from a hand-held air gun created an extremely stable ring combustion zone that could not be extinguished and that was so clean that it was not visible under laboratory light. A blue ring combustion zone was visible when the laboratory lights were switched off.

Under strong blowing, the character of the flame changed from a swirl type long luminous flame to a transparent blue truncated flame ring at the outermost port. The flame ring was approximately one-third to one-half a cylinder diameter in height located near the cylinder wall. No reaction was apparent within the flame ring. The formation of the ring combustion zone appeared to produce a flow pattern in which, after one circulation of the tube, some of the high temperature gases were mixed with the initially unmixed and unreacted fuel and air. No recirculation zone was apparent, and flame stabilization apparently occurred through a mechanism quite different than observed in swirl flames.

The discovery of a flame with these unusual properties was quite intriguing and presented several promising features for gas turbine combustors. The color of the flame provided a visual indication of flame temperature. Earlier research¹⁹ has indicated that soot was not likely to form in flames when the flame temperature was below 1600 K. Since there was no soot luminosity, it was concluded that the ring combustion zone generated under strong blowing was below 1600 K. Indeed, uncorrected thermocouple measurements had shown a peak flame zone

temperature of approximately 1400 K. Since significant thermal NO formation²⁰ does not occur below 1700 K, what had been achieved was a low NOx combustion device. The key was the asymmetry of the fuel injection port with respect to the cylinder axis.

These early experiments provided good indirect evidence that asymmetric injection of fuel into a whirl flame condition could be the basis for a non-premixed low NOx combustor of unusual stability, and led to the design of the combustor discussed in this effort. The objectives for this new research asymmetric combustor became well-defined. First, to confirm the qualitative visual observations from the split-cylinder experiments, the research combustor would feature controlled metering of fuel and air input streams, and techniques to analytically measure combustion products. Second, to achieve higher air flow rates than were possible with the split-cylinder, the combustor was provided with an air supply capacity two orders of magnitude greater than the inlet air flow induced by the original split cylinder. Finally, the combustor would be enclosed to prevent induced air flows from diluting the product stream, and insulated to reduce heat losses through the combustor walls. Note that for this bench scale combustor, the goal was not to reproduce the geometry of the split-cylinder, but rather to construct a device which would permit a thorough, more controlled study of the physics of asymmetric whirl combustion.

DESCRIPTION OF THE EXPERIMENT

The whirl combustion experiments discussed in this paper have used the Princeton Asymmetric Whirl (PAW) Combustor. As shown in Figure 1, the PAW Combustor is a closed horizontal cylinder, 24" in length and with a 3.5" inner diameter, which serves as the combustion chamber. As shown in Figure 2, fuel was injected through ports in a backplate located at the left end of the cylinder. For symmetric injection, methane was introduced at the center of the fuel backplate. For asymmetric injection, methane was introduced at the periphery of the backplate in a manner that the fuel and the air inlet jets intersect. The air inlet port was located just downstream of the fuel inlet backplate, and was oriented to produce a swirling air flow in the combustor. The combustor cylinder, backplate, and exhaust duct were wrapped with an inch thickness of Kaowool insulation.

The exhaust gases were sampled by a stainless steel probe inserted into the exhaust duct of the combustor. The probe was water-cooled to rapidly quench product gases, and more completely preserve the product gas composition which would be expelled to the atmosphere. The composition of the exhaust gas sample was analyzed by an Nicolet Model 550 FTIR. Because methane-air combustion produces such a large amount of water vapor, both the sample transfer line and the FTIR gas cell were heated to 100° C to avoid water vapor condensation.

Note that unlike many other gas sampling analysis systems, this system did not 'dry' the gas sample. Systems which remove water vapor before analysis risk the potential of removing any species, e.g. NO, which are soluble in water. While more difficult to design and construct, the PAW gas sampling system was designed to process and analyze a heated, undried sample – thereby avoiding the biases encountered with drying and leading to a more accurate measure of NO.

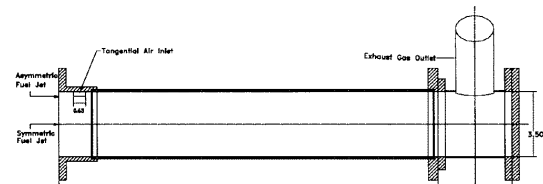


Figure 1. Princeton Asymmetric Whirl Combustor

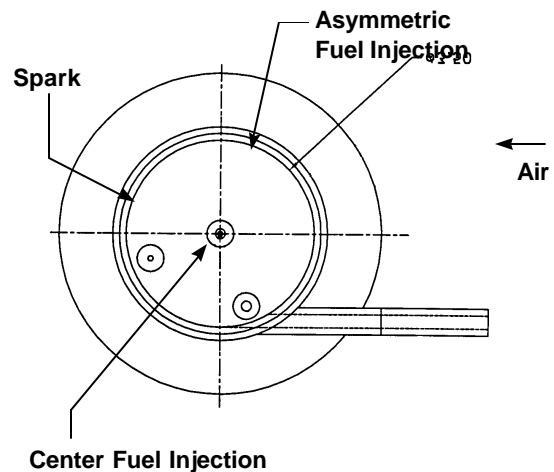


Figure 2. Fuel / Air Injection Ports

EXPERIMENTAL RESULTS

Essential to the explicit characterization of the whirl flame combustor was the experimental mapping of the performance of the combustor over a wide range of fuel-air mixture ratios and whirl flow rates. All experiments reported here were conducted at atmospheric pressure. The results of the experiments are discussed below.

Operating Conditions. The air injection rate was varied over a range from 100 to 200 liters/minute. The methane flow rate was varied from 1 to 4 liters/minute for the lower airflow rate and from 2 to 8 liters/minute for the higher airflow rate. All flow rates were referenced to standard conditions. These conditions corresponded to overall equivalence ratios ranging from $\phi = 0.095$ to 0.38, and adiabatic flame temperatures ranging from 564 K to 1239 K.

It should be stressed that the equivalence ratio reported here is an overall measure of fuel-air mixture which assumes completely uniform mixing between fuel and air. Because the fuel and air are introduced separately into the combustor where mixing and reaction take place, regions will exist within the combustor with local equivalence ratios which are either richer or leaner than the overall equivalence ratio. Of importance is the fact that the lean flammability limit for premixed methane-air flames¹⁸ is reported to occur at $\phi = 0.5$. Clearly, in areas of flame propagation, the local equivalence ratio will be higher than the overall, uniformly-mixed, equivalence ratio.

The range of flow field conditions within the combustor are presented in Table 1 where Q_{air} is the inlet air flow rate, Re is the Reynolds Number computed using the width of the inlet air port, and Fr is the Froude Number.

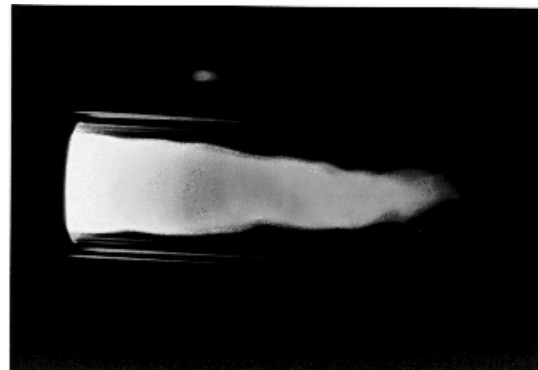
Table 1. Combustor Flow Conditions

Q_{air} (lpm)	100	-	200
$Re_{Air\ Inlet}$	5,800	-	11,600
Fr	5	-	10
Swirl #	17	-	17

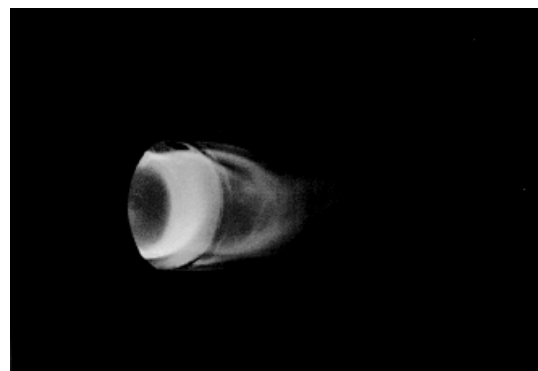
The Reynolds number for the air inlet flow was clearly in the turbulent regime. The Froude number, a measure of the ratio of inertial forces to buoyancy forces, indicated that, at these flow conditions, buoyancy was not a dominant factor in the behavior of this device. The calculated $Fr = V_{\theta} / \pi / \sqrt{g D}$ assumed V_{θ} to be equal to the circumferential velocity and D to be equal to the inner diameter of the combustor. The swirl number calculated was the ratio of the axial flow of circumferential momentum to the axial flow of axial momentum. Typically, swirl combustors have swirl numbers on the order of 0.5-0.7. Systems with swirl numbers above 1 were nominally considered to have high swirl^{9,10}. The whirl combustor has swirl numbers which greatly exceed unity. Clearly, in contrast to conventional swirl combustors, the combustor evaluated was characterized by circumferential velocities which greatly exceeded axial velocities.

Visual Observations. Figure 3 presents photographs of two whirl flames produced by injecting 200 liters/minute of air and 6 liters/minute of methane into the combustor. The overall equivalence ratio for both was $\phi=0.286$. Centerline injection of fuel produced an elongated, highly luminous, orange flame from 3-4 combustor diameters in length. However, by simply shifting the location of the fuel inlet to the periphery of the backplate, a blue, virtually non-luminous flame, only a single combustor diameter in length, was produced. In fact, the asymmetric whirl flame was not visible in a lighted laboratory. These differences in the flame structure are all the more

unusual in view of the fact that neither the air nor fuel inlet rates were altered to produce this effect.



(a) Symmetric Fuel Injection



(b) Asymmetric Fuel Injection

Figure 3. Comparison of Symmetric and Asymmetric Fuel Injection

In both cases, the flames, when viewed end-on, appeared to have a hollow central region with a distributed reaction zone approximately 1/2 cm from the wall. No reaction was visible within the large hollow central core of the flames. These observations were consistent with Hottel's early symmetric fuel-injected whirl flame experiments¹¹ and with our split-cylinder whirl flame results⁸.

Emissions as a Function of Overall Equivalence Ratio. Exhaust gas mole fractions of NO, NO₂, CO, and unburned CH₄ for the baseline combustor configuration were measured and are presented in Figures 4 to 8 for equivalence ratios ranging from 0.095 to 0.38. Following the standard practice for reporting emissions from gas turbines, all emissions were corrected to 15% O₂ in the product stream.

As shown in Figure 4, NO levels increased monotonically as equivalence ratio increased. For $Q_{air}=100$ liters/minute, NO increased from sub-PPM levels at $\phi = 0.095$ to 23 PPM at $\phi = 0.38$, and was primarily a temperature effect. NO production by the

Zeldovich mechanism is highly temperature sensitive²⁰. The adiabatic flame temperature for lean fuel-air mixtures rose from 564 to 1389 K as the overall equivalence ratio was increased from $\phi = 0.095$ to 0.38. NO formed by the Zeldovich mechanism accelerated as ϕ increased.

In lean combustion of hydrocarbons in air, nitrogen dioxide can make up a significant fraction of the nitrogen oxides produced as a reaction by-product²¹. As seen in Figure 5, NO₂ emissions increased as equivalence ratio increased from $\phi = 0.095$ to $\phi = 0.2$, and then declined as equivalence ratio was further increased from $\phi = 0.2$ to $\phi = 0.38$. At the low temperatures associated with the leanest fuel-air mixtures, little NO was produced for conversion to NO₂. As equivalence ratio increased, sufficiently high concentrations of HO₂ became available to convert NO to NO₂. However, at even higher equivalence ratios, sufficiently high concentrations of the radical species, OH, H, and O atom, were produced for rapid destruction of NO₂ to form NO.

NOx as a function of ϕ is shown in Figure 6. For Q_{air}=100 liters/minute, NOx < 15 PPM was achieved for $\phi < 0.18$. For the same inlet air flow, NOx < 25 PPM for $\phi < 0.38$. Several researchers have reported that rapid quenching of combustion gases in sample probes can permit the conversion of NO to NO₂ - both in the gas phase and on the probe walls^{22,23,24}. Combination of NO and NO₂ into a NOx total provided a summary measure of all major nitrogen oxides regardless of their formation route.

Because both NO formation and fuel oxidation are temperature dependent, there was a tradeoff between lower NO and increased CO and CH₄ emissions. As seen in Figures 7 and 8, CO and CH₄ mole fractions were quite high for the leanest mixtures investigated measuring 230 PPM and 1389 PPM respectively at $\phi = 0.095$ at 15% O₂ for the lowest air inlet rate. However, as ϕ (and flame temperature) were increased, CO and fuel oxidation rates accelerated, and both CO and fuel emission levels declined. At 100 lpm, essentially complete consumption of CH₄ was achieved by $\phi = 0.28$. CO levels fell under 3 PPM by $\phi = 0.38$.

CO oxidation to CO₂ can be quenched through a number of routes including quenching at a cool wall surface²⁵. In the PAW Combustor, the flame zone is located in the turbulent shear layer quite close to the combustor wall. When compared with the combustion temperature, the temperature of the quartz combustor wall was comparatively cool. Combustor outside wall temperatures were in the range of 400 K to 750 K depending upon the fuel-air mixture. The inner wall

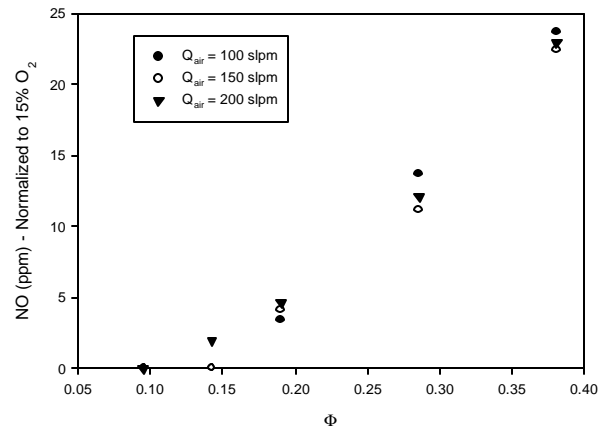


Figure 4. NO Emissions as a function of Equivalence Ratio. Insulated Combustor with No Air Preheat.

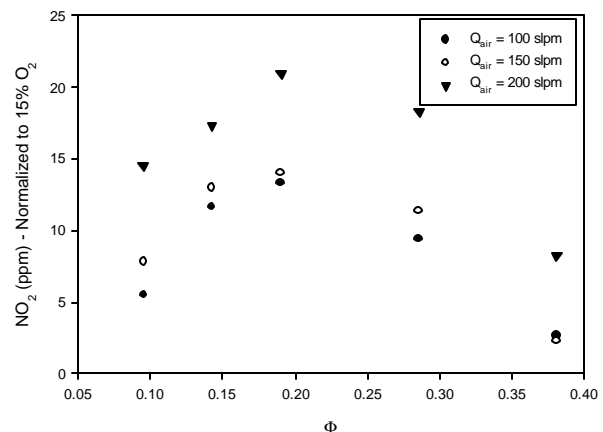


Figure 5. NO₂ Emissions as a function of Equivalence Ratio. Insulated Combustor with No Air Preheat.

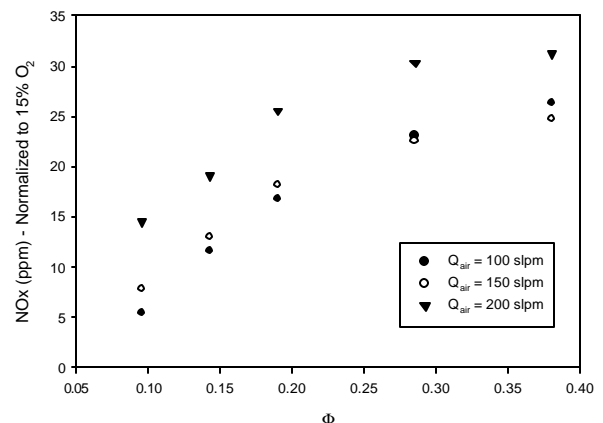


Figure 6. NOx Emissions as a function of Equivalence Ratio. Insulated Combustor with No Air Preheat.

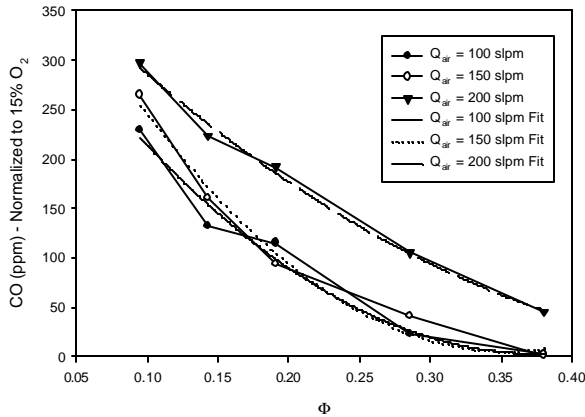


Figure 7. CO Emissions as a function of Equivalence Ratio. Insulated Combustor with No Air Preheat.

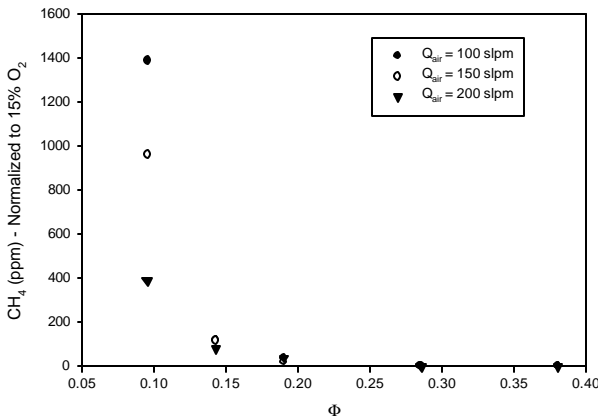


Figure 8. Unburned CH₄ Emissions as a function of Equivalence Ratio. Insulated Combustor with No Air Preheat.

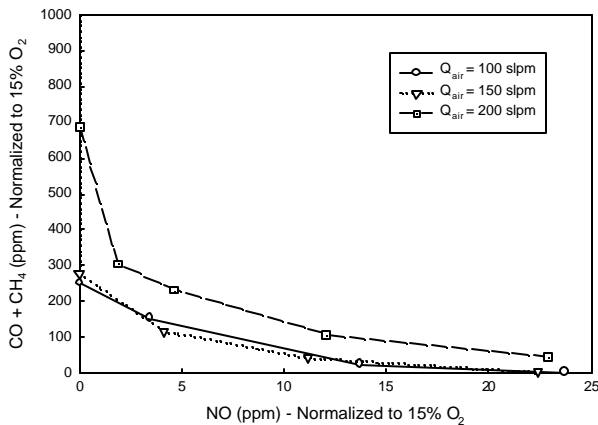


Figure 9. CO vs. NO Emissions for three different Air Inlet Flow Rates. Insulated Combustor with No Air Preheat.

temperatures were below 1300 K – the devitrification point of fused quartz. CO oxidation reaction rates are highly temperature dependent, and significant oxidation of CO does not occur for temperatures below 1100 K^{18,26,27}. CO conversion to CO₂ would be quenched for any CO transported to the cool combustor wall by turbulent eddies.

NO and combined CO/CH₄ emissions data have been replotted in Figure 9 to show the tradeoff between the two exhaust components. Because both fuel oxidation and NO formation rates are temperature sensitive, conditions which lead to low NO were expected to result in higher combined CO/CH₄ emissions and vice versa. This tradeoff is clearly seen in Figure 9. Note however that NO emissions below 15 PPM were achieved at $\phi = .28$ with CO emissions below 25 PPM at 15% O₂. The diagram also shows that the effect of CO quenching at higher flow rates was to shift the NO-CO/CH₄ curve vertically to higher CO levels while maintaining constant NO emissions.

In addition to the strong relationship between equivalence ratio and emissions levels, the data also indicated that air flow rate had a measurable effect upon emissions levels. A number of factors linked the flow field to the combustor performance. Specifically, increased air injection rate (1) decreased combustor residence time, and (2) increased turbulent intensity and the rate of turbulent mixing. Higher rates of turbulent mixing could lead to lower NO as the consequence of improved fuel-air mixing, but could also act to quench the slow process of CO oxidation as cooler eddies interacted with eddies transporting higher temperature CO and O₂ from the flame.

Minimizing Emissions with Preheated Inlet Air.

Figure 9 demonstrated the fundamental tradeoff between CO emissions and NOx emissions. As both CO oxidation and NO formation rates were highly temperature dependent, operating conditions which minimized one species tended to aggravate levels of the other species. However, chemical kinetic studies of the two species have suggested that there may exist a temperature regime between 1100 K, the threshold for CO oxidation²⁷, and 1700 K, the threshold for NO formation²⁰, which could promote burnout of CO without significant acceleration of NO formation rates.

To evaluate the opportunity for operation in this regime, an experimental series was designed which preheated the inlet air by 125°C, and measured emissions as a function of equivalence ratio. The hypothesis was that, under low temperature, ultra-lean operating conditions, even a small amount of preheat could produce significant reductions in CO with little increase in NOx emissions. Figures 10 to 14 compare the results of the experiments with preheat with the results of the experiments without preheat presented earlier. All experiments in this sequence were

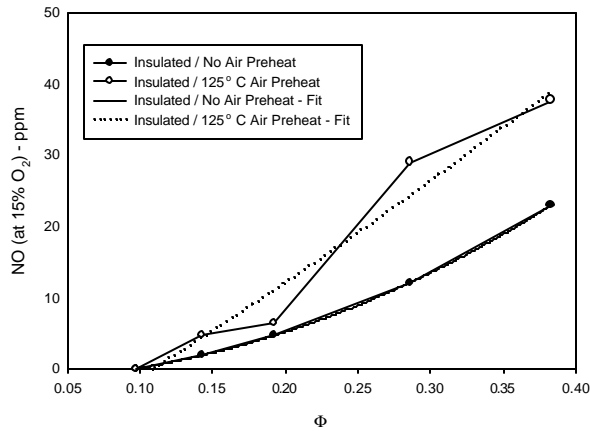


Figure 10. NO Emissions vs. Equivalence Ratio for Inlet Air with and without Preheat. Air Inlet Flow Rate = 200 liters / minute.

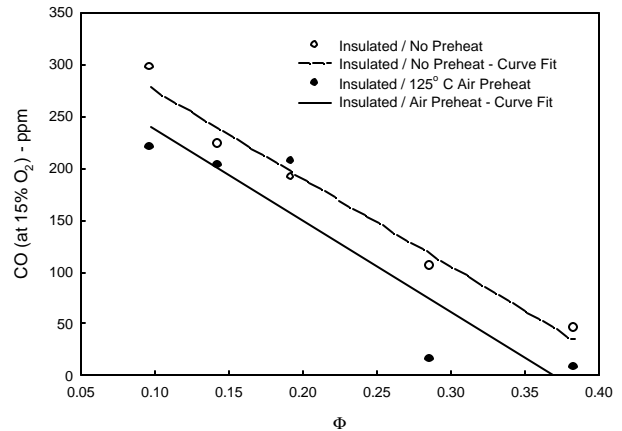


Figure 13. CO Emissions vs. Equivalence Ratio for Inlet Air with and without Preheat. Air Inlet Flow Rate = 200 liters / minute.

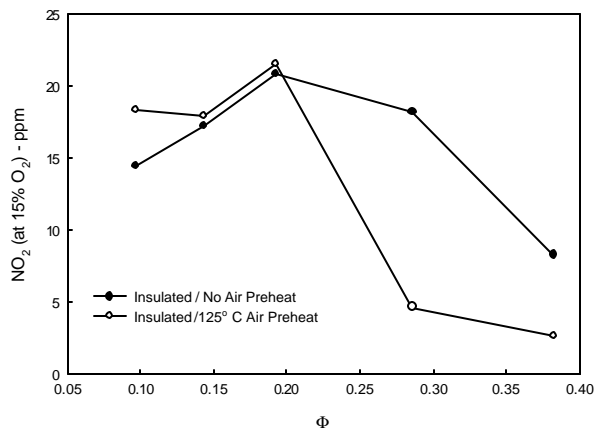


Figure 11. NO₂ Emissions vs. Equivalence Ratio for Inlet Air with and without Preheat. Air Inlet Flow Rate = 200 liters / minute.

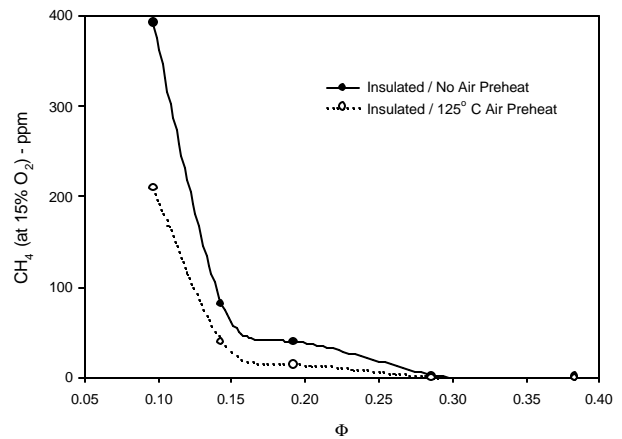


Figure 14. Unburned CH₄ vs. Equivalence Ratio for Inlet Air with and without Preheat. Air Inlet Flow Rate = 200 liters / minute.

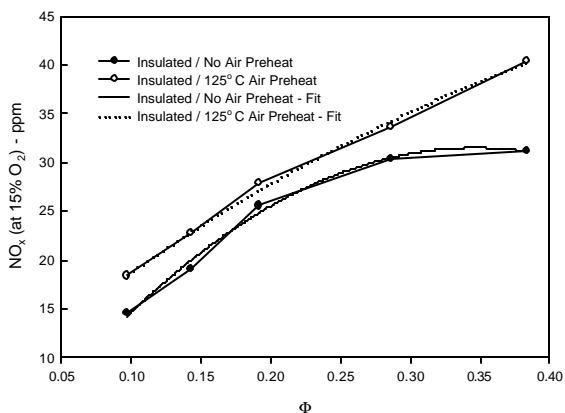


Figure 12. NO_x Emissions vs. Equivalence Ratio for Inlet Air with and without Preheat. Air Inlet Flow Rate = 200 liters / minute.

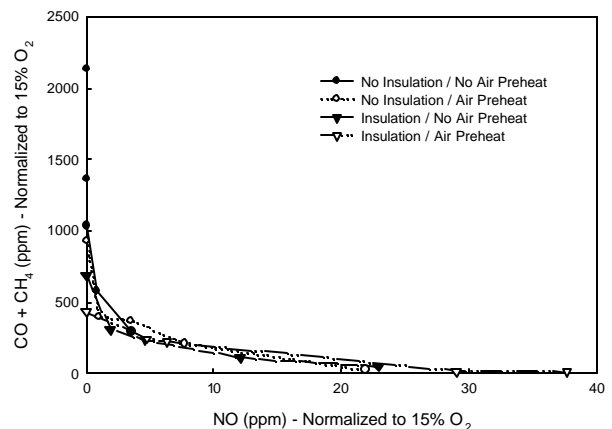


Figure 15. NO vs. CO+CH₄ Emissions as a function of Air Preheat and Non-Insulated Combustor Wall Losses. Air Inlet Flow Rate = 200 liters/minute.

conducted with an air inlet flow rate of 200 liters / minute referenced to standard conditions. The fuel was methane. Inlet air temperature in cases without preheat was $T_{\text{air}} = 287$ K, while temperature in cases with preheat was $T_{\text{air}} = 411$ K for an incremental preheat of approximately 125° C.

Note that 125° C of preheat has a favorable effect for $\phi < 0.25$. For these conditions, little difference was noted between NO, NO₂, or NOx emissions with or without preheat while CO emissions over this same range declined by approximately a third and unburned CH₄ emissions decreased by about a half. Note however that for $\phi > 0.25$, preheating continues to decrease CO emissions, but only at expense of a near doubling in NO emissions and a 25% increase in NOx emissions – reflecting the high sensitivity of NO formation to reaction temperature.

Figure 15 presents incompletely reacted fuel (CO + CH₄) vs. NO emissions measurements for four asymmetric whirl combustor configurations: (1) Insulated Combustor with 125° C air preheat, (2) Insulated Combustor with no air preheat, (3) Cold, uninsulated walls with 125° C air preheat, and (4) Cold, uninsulated walls with no air preheat. The data for all four configurations appeared to collapse onto a single curve clearly showing that in this combustor CO emissions were inversely proportional to NO emissions. The slope of this curve is steepest for the lean equivalence ratios which favor low NO – illustrating why preheating for very lean mixtures can produce large reductions in CO with only small incremental increases in NO. Conversely, the slope of the curve approaches zero for the richer equivalence ratios which favor higher NO – indicating that preheat produces an increasingly less favorable tradeoff between NO and CO as equivalence ratio increases in lean mixtures.

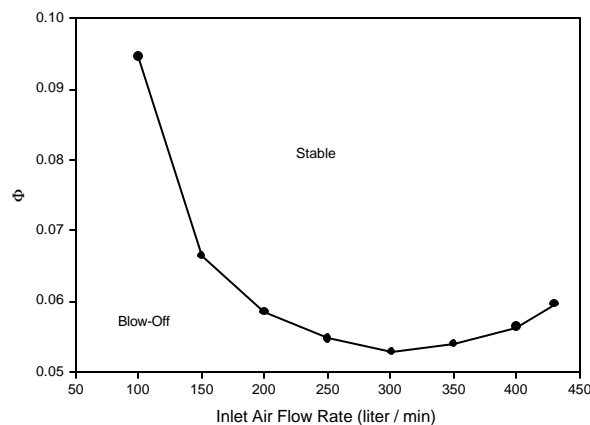


Figure 16. Whirl Combustor Lean Blow Off Limits. Methane Fuel. Insulated Combustor.

Lean Blow Off. Early experiments with buoyancy-induced whirl flames⁸ suggested that off-axis fueled whirl flame have an unusual resistance to flame blow-off. A series of blow-off experiments was

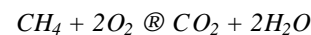
conducted with the PAW to ascertain the fuel lean blow-off limits of this combustor. Figure 16 shows the results of a series of experiments in which air inlet flow rate was fixed at a number of settings and fuel injection was gradually reduced until flame extinction occurred. As with the split cylinder, the flame within the PAW was unusually stable. Blow-off occurred typically at $\phi < 0.1$ overall. By comparison, the lean flammability limit for a premixed methane air flame is $\phi = 0.5$.

NUMERICAL MODELING OF WHIRL FLAME STRUCTURE

The key to understanding the remarkable performance of this combustion concept was to understand the physics and internal structure of asymmetrically-fueled whirl flames. Intrusive measurement of the internal flame properties with thermocouples and sampling probes was found to disrupt the delicate features of the flame, and was, limited, in any case, to the specific geometry of the bench scale combustor. To explore the internal flow field and reaction rate distribution within the flame, a numerical model of the whirl combustor was developed using finite-difference discretization of the Reynolds-averaged governing equations of mass, momentum, enthalpy, and species conversation²⁸.

Description of the Numerical Model. The combustor was represented as a horizontal axisymmetric cylinder of 4 diameters in length having azimuthal symmetry. In the numerical experiment, air was injected at one end of the cylinder with a strong tangential velocity component (33.8 m/s) and fuel was introduced near the wall with an axial-only velocity component (5.6 m/s). The case presented here was for a whirl flame produced by injecting 200 liters / minute of air and 6 liters / minute of methane into the combustor. Overall equivalence ratio for this condition is $\phi = 0.286$. Inlet temperatures were set at 300K.

The model assumed single step oxidation of methane with oxygen to form carbon dioxide and water vapor:



The reaction rate for this single step used the global one-step methane oxidation reaction rate proposed by Westbrook and Dryer²⁹ to determine laminar flame speeds for premixed flames in standard SI units:

$$dCH_4/dt = -130 \times 10^6 \exp(-24400/T) [CH_4]^{-0.3} [O_2]^{1.3}$$

Note that one limitation of this model was the one-step methane-air reaction mechanism which does not allow for dissociation of combustion products. However, since the major energy release is the oxidation of CO to CO₂, this model should be appropriate for analyzing temperature fields.

With an inlet air flow rate of Re=11,600 based on the air inlet diameter, the flow field was considered

turbulent. The Renormalization Group $k-\epsilon$ turbulence model was used to represent the turbulent sub-grid scales. The eddy-breakup model as formulated by Magnussen and Hjertager was used to model turbulence-chemistry interactions³⁰. The model incorporated complete temperature and composition dependent transport and thermal properties.

To model the combustor as an axisymmetric device, the fuel was introduced into the combustor model through an annulus located at the same radius as the physical fuel port with a width chosen to preserve the axial momentum of the fuel jet. Likewise, air inlet flow was distributed circumferentially such that the inlet mass flow rate in the radial direction and the inlet circumferential momentum flow rate were preserved. The volume of the combustor was discretized into a grid of 82 cells in the radial direction and 84 cells in the axial direction. The layout of the grid was designed such that spatial resolution was greatest in the areas where mixing was expected to occur, e.g., near the fuel and air inlet ports, and where velocity gradients were expected to be steepest, e.g., near the wall. Combustor walls are modeled as adiabatic boundaries.

Results of Reacting Flow Simulation. To examine the structure of the reacting flow within the combustor, contours of the temperature field, the flow field, the turbulent kinetic field, and the reaction rate distribution were computed and are discussed below.

Flow Field. Because the air flow is two orders of magnitude higher than the fuel flow, the air flow controls the flow field, and the fuel injection stream introduces only a perturbation in the overall flow field. Figure 17 presents the calculated flow velocity field within the combustor. The flow field is clearly composed of two relatively distinct flow zones - as noted in experiments with the PAW combustor. The first zone along the wall of the combustor is the primary flow path for air entering from the air inlet and exiting the combustor at the exhaust point. Flow within this outer zone is highly turbulent and maintains a large fraction of the swirling velocity component introduced at the air inlet. The second zone, a large central core, occupies approximately 80% of the diameter of the combustor. Flow within the central core is relatively stagnant compared to the strong turbulent flow along the walls.

Turbulence Field. The turbulence created at the boundary of the two flow zones should have a large and potentially controlling influence on combustion rates. Figure 18 illustrates the distribution of turbulent kinetic energy, $\frac{1}{2} u'^2$ where u' = the root mean square of the turbulent velocity fluctuation. Turbulent kinetic energy is at a maximum in the shear layer created by the inlet air jet. Because turbulent mixing of methane and air is much more rapid than the rate of diffusive fuel-air mixing, injection of fuel directly into this shear layer should minimize fuel-air mixing time, and the

conditions created should approach that of pre-mixed combustion rather than that controlled by diffusion.

Distribution of Reaction Rate. To pursue the theory that turbulent mixing controls the reaction rates within the PAW combustor, the single-step reaction rates for the two models were examined. As shown in Figure 19, off-axis injection of fuel introduces fuel directly into the shear layer created by the incoming air stream upon entry into the combustor. The model for this combustor configuration predicts a short distributed flame zone of roughly one diameter in length. This prediction is in agreement with the observed spiral-like flame zone noted in the experimental tests.



Figure 17. Flow Field: Axial and Radial Resultant Velocities. $Q_{\text{air}} = 200$ liters/min., $Q_{\text{CH}_4} = 6$ liters /min., $f=0.286$. Maximum velocity = 7.0 m/s.

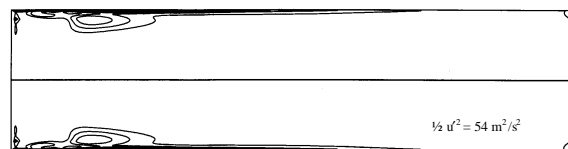


Figure 18. Distribution of Turbulent Kinetic Energy: $Q_{\text{air}} = 200$ liters/min., $Q_{\text{CH}_4} = 6$ liters /min., $f=0.286$. Peak turbulent kinetic energy = $54 \text{ m}^2/\text{s}^2$.

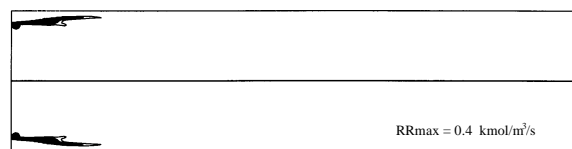


Figure 19. Distribution of Reaction Rate, $\text{CH}_4 + \text{O}_2 \rightarrow \text{CO}_2 + 2 \text{H}_2\text{O}$: $Q_{\text{air}} = 200$ liters/min., $Q_{\text{CH}_4} = 6$ liters /min., $f=0.286$. Max reaction rate = $0.4 \text{ kmol}/\text{m}^3/\text{s}$.

Pressure and Velocity Radial Profiles. Figure 20 presents the radial profile of the flow field and pressure at an axial location just downstream of the air inlet port ($z / D = 0.37$). Note that the strong tangential component of velocity produces a pressure gradient with low pressures in the center of the cylinder and higher pressures at the wall. The pressure gradient is required to balance the centrifugal forces exerted on a swirling fluid element. As observed by Hottel, the tangential velocity, w , profile forms two zones. The outer portion is characterized by a free vortex flow ($w \sim 1/r$) while the inner portion is characterized by solid

rotation ($w \sim r$). The reaction zone appears to be located in the turbulent shear layer where the two zones intersect. As seen in the plot of axial velocity, u , the bulk of the axial flow occurs near the wall where excess air and combustion products are swept from the cylinder. The interior is relatively quiescent with only limited recirculation, or reverse flow, occurring between $r/R = 0.3$ and $r/R = 0.6$.

Species Radial Distribution. Under the radial pressure gradient across the cylinder, gases which are lighter, e.g., hot combustion products, are preferentially drawn toward the center of the combustor. Figure 21 presents the distribution of species at $z/D = 0.37$, and clearly shows that the hot combustion products CO_2 and H_2O accumulate in the center core of the combustor. Reflecting the stoichiometry of CH_4 - air reaction, H_2O and CO_2 are found in approximately a 2:1 ratio. CH_4 exists in small quantities near the wall at approximately the same radius where fuel injection originally took place. As expected, the mole fraction of molecular oxygen declines with distance from the wall as O_2 reacts with the fuel. Note that as the model uses only a global single chemical mechanism, the only combustion products modeled are CO_2 and H_2O . Future work will extend this model to investigate the distribution of other products, e.g., CO and NO_x .

The combination of tangential injection of air and tangential exit of combustion products appears to create a low pressure trough along the centerline of the combustor extending from the centerline to $r \approx 0.8 R$. In agreement with the numerical model, the Rayleigh Criterion predicts that hot, low-density combustion product gases are trapped in this trough. This hot central core stabilizes the flame by acting as a source of enthalpy and radicals.

Internal Temperature Distribution. Note that the temperature of the center core is on the order of 1900K. This is significantly higher than the adiabatic flame temperature of 1032 K for this fuel-air mixture of $\phi = 0.286$. Experimental measurements of axial centerline temperature confirm that the centerline temperature does indeed exceed the adiabatic flame temperature. Axial temperature measurements of an uninsulated combustor, which is subject to both radiative and convective heat losses and should be cooler than an adiabatic combustor, show a peak centerline temperature of 1300 K for $\phi = 0.286$.

The region which exceeds the adiabatic flame temperature extends over 80% of the combustor volume, and both visually and in the numerical simulation is undergoing no apparent chemical reaction. The reason for this phenomenon is unclear, but would appear to occur as the result of some fraction of the hot combustion products being captured within the central core zone by the radial pressure gradient across the combustor. If these combustion products were formed by reaction of fuel and air at more fuel rich proportions,

the combustion products would be at temperatures higher than the overall adiabatic flame temperature.

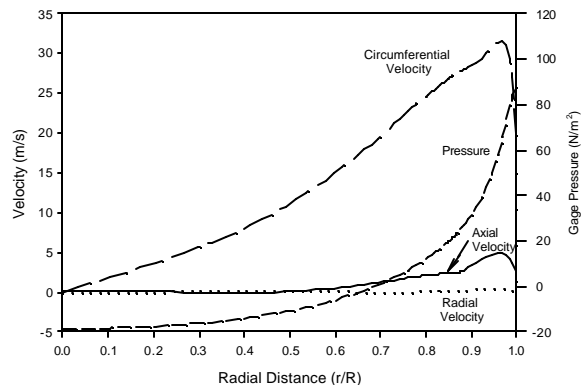


Figure 20. Flow Field and Radial Pressure Distribution at Axial Location at downstream edge of air inlet: $Q_{\text{air}} = 200$ liters/min., $Q_{\text{CH}_4} = 6$ liters /min., $f=0.286$.

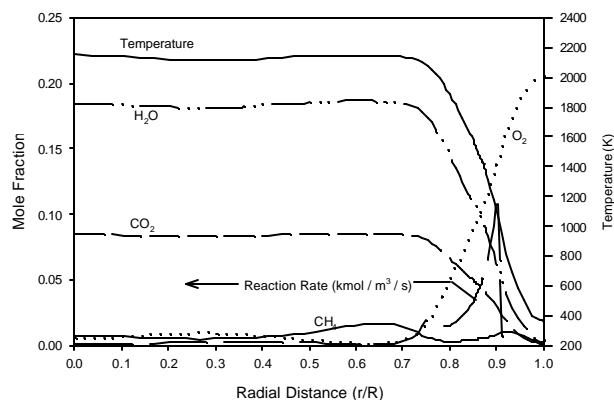


Figure 21. Radial Species Distribution: $Q_{\text{air}} = 200$ liters/min., $Q_{\text{CH}_4} = 6$ liters /min., $f=0.286$.

CONCLUSIONS

Asymmetrically-fueled whirl flames hold great promise as the foundation for a new generation of low- NO_x combustor designs. The combustor concept introduces fuel and air separately which avoids the dangers and complexity of lean pre-mixed combustion. Experiments have shown the combustor to exhibit unusual stability even for equivalence ratios below $\phi=1$. Both numerical modeling and thermocouple measurement have demonstrated the existence of a quiescent zone in the center of the cylinder which is composed of combustion products and exists at a temperature which exceeds the adiabatic flame temperature. Experiments with this laboratory scale burner have recorded NO emissions below 15 PPM with associated CO levels of 25 PPM. These are remarkably low emissions levels for a bench-scale combustor, and strongly suggest the potential for even larger reduction in thermal NO_x emission levels in asymmetrically-fueled whirl combustors optimized for large scale gas turbines.

REFERENCES

- ¹Bathie, W.W. *Fundamentals of Gas Turbines*, 2nd Ed., John Wiley & Sons, New York (1996).
- ²Valenti, M. "Breaking the Thermal Efficiency Barrier", *Mechanical Engineering*, pp. 86-89, (July 1995).
- ³Valenti, M. "Combined-Cycle Plants: Burning Cleaner and Saving Fuel", *Mechanical Engineering*, pp. 46-50, (September 1991).
- ⁴South Coast Air Quality Management District (SCAQMD), Rule 1134 as amended 12/7/95. "Emissions of Oxides of Nitrogen from Stationary Gas Turbines".
- ⁵Bowman, C.T., "Control of Combustion-Generated Nitrogen Oxide Emissions: Technology Driven by Regulations," *Twenty-Fourth Symposium (International) on Combustion*, The Combustion Institute, Pittsburgh, pp. 859-878 (1992).
- ⁶Doebbling, K., Knopfel, H.P., Polifke, W., Winkler, D., Steinback, C., and Sattelmayer, T., "Low-NO_x Premixed Combustion of MBtu Fuels Using the ABB Double Cone Burner (EV Burner)," *Transactions of the ASME Journal of Gas Turbines and Power*, v. 118, pp.46-53 (1996).
- ⁷Snyder, T.S., Rosfjord, T.J., McVey, J.B., Hu, A.S., and Schlein, B.C., "Emission and Performance of a Lean-Premixed Gas Fuel Injection System for Aeroderivative Gas Turbine Engines," *Transactions of the ASME Journal of Gas Turbines and Power*, Vol 118, pp.38-45 (1996).
- ⁸Glassman, I., Yetter, R., Gabler, H.C., and Sivo, J., "Asymmetric Whirl Combustion: A New Phenomenon?", *Proceedings of the 1994 Fall Technical Meeting of the Eastern States Section of the Combustion Institute*, Clearwater Beach, FL (1994).
- ⁹Beer, J.M. and Chigier, N.A., *Combustion Aerodynamics*, John Wiley & Sons, Inc., New York (1972).
- ¹⁰Gupta, A.K., Lilley, D.G., and N.Syred, *Swirl Flows*, Abacus Press (1984).
- ¹¹Hottel, H.C. and Person, R.A. "Heterogeneous Combustion of Gases in a Vortex System", *Fourth Symposium (International) on Combustion*, pp. 781-788 (1953).
- ¹²Albright, L.F. and Alexander, L.G. "Flame Stabilization in Gases Flowing Cyclonically: Flow Characteristics, Temperatures, and Gas Analyses", *Fifth Symposium (International) on Combustion*, The Combustion Institute, Pittsburgh, pp. 464-472 (1956).
- ¹³Ishizuka, S., "On the Behavior of Premixed Flames in a Rotating Flow Field: Establishment of Tubular Flames", *Twentieth Symposium (International) on Combustion*, The Combustion Institute, Pittsburgh, PA, pp. 287-294 (1984).
- ¹⁴Gupta, A.K., Beer, J.M., and Swithenbank, J., "Concentric Multi-Annular Swirl Burner: Stability Limits and Emission Characteristics", *Sixteenth Symposium (International) on Combustion*, The Combustion Institute, Pittsburgh, PA, pp. 79-91 (1976).
- ¹⁵Ahmad, N.T., Andrews, G.E., Kowkabi, M., and Sharif, S.F., "Centrifugal Mixing Forces in Enclosed Swirl Flames", *Twentieth Symposium (International) on Combustion*, The Combustion Institute, Pittsburgh, PA, pp. 259-267 (1984).
- ¹⁶Emmons, H.W. and Ying, S.-J., "The Fire Whirl", *Eleventh Symposium (International) on Combustion*, The Combustion Institute, Pittsburgh, p.475 (1967).
- ¹⁷Chigier, N.A., Beer, J.M., Grecov, D., and Bassindale, K., "Jet Flames in Rotating Flow Fields," *Combustion and Flame*, v. 14, pp. 171-180 (1970).
- ¹⁸Glassman, I., *Combustion*, 3rd Ed., Academic Press, New York (1996).
- ¹⁹Glassman, I., Nishida, O., and Sidebotham, G., "Critical Temperatures of Soot Formation", pp. 316-321, *Soot Formation in Combustion: Mechanisms and Models*, Springer-Verlag, New York (1994).
- ²⁰Miller, J.A. and Bowman, C.T. "Mechanism and Modeling of Nitrogen Chemistry in Combustion", *Progress in Energy and Combustion Science*. v. 15, 287-388 (1989).
- ²¹Johnson, G.M. and Smith, M.Y. "Emissions of Nitrogen Dioxide from a Large Gas-Turbine Power Station", *Combustion Science and Technology*, v. 19, p. 67-70 (1978).
- ²²Ceransky, N.P. and Sawyer, R.F. "NO and NO₂ Formation in a Turbulent Hydrocarbon / Air Diffusion Flame," *Fifteenth Symposium (International) on Combustion*, The Combustion Institute, Pittsburgh, Pa, pp. 1039-1050 (1975).
- ²³Allen, J. D. "Probe Sampling of Oxides of Nitrogen from Flames," *Combustion and Flame*, v. 24, pp. 133-136 (1975).
- ²⁴Levy, A. "Unresolved Problems in SO_x, NO_x, Soot Control in Combustion", *Nineteenth Symposium (International) on Combustion*, The Combustion Institute, Pittsburgh, PA, pp. 1223-1242 (1982).
- ²⁵Correa, S.M. "Carbon Monoxide Emissions in Lean Premixed Combustion", *Journal of Propulsion and Power*, v. 8, No. 6, pp. 1144-1151 (1992).
- ²⁶Dryer, F.L., Naegli, D.W., and Glassman, I., "Temperature Dependence of the Reaction CO + OH = CO₂ + H", *Combustion and Flame*, v. 17, p. 270-272 (1971).
- ²⁷Yetter, R.A., Dryer, F.L., and Rabitz, H. "A Comprehensive Reaction Mechanism for Carbon Monoxide / Hydrogen / Oxygen Kinetics", *Combustion Science and Technology*, v. 79, pp. 97-128 (1991).
- ²⁸*Fluent User's Guide*, Release 4.4, Fluent Incorporated, Lebanon, NH (1996).
- ²⁹Westbrook, C.K. and F.L. Dryer, "Simplified Reaction Mechanisms for the Oxidation of Hydrocarbon Fuels in Flames," *Combustion Science and Technology*, v. 27, pp 31-43 (1981).
- ³⁰Magnussen, B.F. and Hjertager, B.H., "On Mathematical Modeling of Turbulent Combustion with Special Emphasis on Soot Formation and Combustion", *Sixteenth Symposium (International) on Combustion*, The Combustion Institute, Pittsburgh, PA, pp. 719-729 (1976).